Oxidative Stress Impact on Barrier Function of Porcine Angular Aqueous Plexus Cell Monolayers

Yuan Lei,[1] William D. Stamer,[2] Jihong Wu,[1] and Xinghuai Sun[3]

[1]Research Centre, Eye and ENT Hospital of Fudan University, Shanghai, China
[2]Department of Ophthalmology, Duke University, Durham, North Carolina
[3]Department of Ophthalmology, Eye and ENT Hospital of Fudan University, Shanghai, China

Correspondence: Xinghuai Sun, Department of Ophthalmology, Eye and ENT Hospital of Fudan University, Shanghai, 200031 China; xhsun@shmu.edu.cn.

Submitted: December 4, 2012
Accepted: May 30, 2013

Citation: Lei Y, Stamer WD, Wu J, Sun X. Oxidative stress impact on barrier function of porcine angular aqueous plexus cell monolayers. *Invest Ophthalmol Vis Sci*. 2013;54:4827–4835. DOI:10.1167/iovs.12-11435

Purpose. Our goal was to investigate the effect of chronic oxidative stress on angular aqueous plexus (AAP, functional equivalent to human Schlemm's canal) endothelial cells from porcine eyes.

Methods. AAP cells were differentially isolated from porcine outflow tissues using puromycin selection. Confluent cultures of porcine AAP cells were grown for 2 weeks in physiological (5% O_2) or hyperoxic conditions (40% O_2) to model elevated oxidative stress associated with ageing. Cell growth rate, size, transendothelial electrical resistance (TEER), and hydraulic conductivity (HC) were measured. The expression of senescence-associated β-galactosidase and DNA damage marker 8-hydroxy-2′-deoxyguanosine (8-OHdG) was monitored, and the levels of cytoskeletal and cell–cell adhesion proteins such as F-actin, phospho-myosin light chain (phosphor-MLC), occludin, claudin-5, ZO-1, β-catenin, and VE-cadherin were measured by immunofluorescence staining and Western blot analysis.

Results. Data showed that chronic hyperoxia inhibited cell growth rate from day 3 onward, the cell size increased by 18.2% ± 5.1%, and cells stained positive for β-galactosidase and 8-OHdG. Hyperoxia resulted in a significant 30% increase in TEER compared with the control group ($P < 0.05$, $n = 6$). When perfused in the basal-to-apical direction at 4 mm Hg, HC of AAP cells was 1.97 ± 0.12 and 1.54 ± 0.13 μL/mm Hg/min/cm^2 in control and hyperoxia groups, respectively ($P < 0.05$, $n = 6$). Stressed cells expressed a significantly greater abundance of F-actin, phospho-MLC, occludin, claudin-5, β-catenin, and VE-cadherin compared to the control group by both immunofluorescence and Western blot analyses.

Conclusions. Chronic exposure of AAP cells to oxidative stress decreased cell monolayer permeability and up-regulated cytoskeletal and cell–cell adhesion protein expression; suggesting that, with age and increased oxidative stress, resistance at the level of Schlemm's canal increases.

Keywords: glaucoma, Schlemm's canal endothelial cells, ageing

Glaucoma affects approximately 80 million people worldwide[1] and is characterized by cupping of the optic nerve head and irreversible loss of retinal ganglion cells. Ageing and elevated intraocular pressure (IOP) are the two major risk factors for developing primary open angle glaucoma (POAG).[2–8] Increased resistance at the level of the conventional outflow pathway is responsible for elevated IOP in POAG. During cell metabolism, oxidizing species or reactive oxygen species (ROS) are continuously being produced. When a greater amount of oxidizing species are produced or not neutralized, they may consequently cause molecular damage and, over time, trabecular or Schlemm's canal (SC) endothelial cell dysfunction[9,10] and elevation in outflow resistance, ultimately increasing the risk of the disease.

The SC inner wall is formed by endothelial cells whose interaction with juxtacanalicular trabecular cells and barrier function is thought to be important in controlling outflow resistance and thus IOP, making it one of the key tissues to study to better understand the etiology of ocular hypertension in glaucoma.[11,12] The SC inner wall endothelium forms a continuous layer of endothelial cells, which is the barrier to aqueous humor entry from the juxtacanalicular space into the SC canal lumen.[13,14] Human SC endothelial cells are long and slender with their long axis parallel to direction of flow along the canal lumen. Tight junctions and desmosomes join the cells to one another and form a continuous region of contact. Thus, the main source of outflow resistance and "extra" resistance in glaucoma is thought to be in the near vicinity of the inner wall endothelium of SC. Moreover, modulation of SC cell junctions, morphology, and contractile characteristics have been reported to influence hydraulic conductivity of SC cells[13] and outflow facility in perfused eyes.[14]

Our hypothesis is that chronic oxidative stress of SC cells leads to reduction in its permeability, which is due to an alteration in the structure and organization of cytoskeleton and junction proteins. To test this hypothesis we used porcine angular aqueous plexus (AAP) cells as a model for human SC cells and chronic hyperoxia as a model for chronic oxidative stress associated with ageing. We employed an established model of chronic oxidative stress that has been used to study

the effects of continuous low level oxidative stress on many cells including trabecular meshwork (TM) cells.[15] This model is preferred by others because it provides a constant increase of reactive oxygen species without the need of additional chemical or cellular treatments.[16–18] In addition, this model has relatively low toxicity in that sustained confluence and thus normal postmitotic conditions were assured throughout the length of the experiment.[19] Oxidative stress is one of the major contributors to the ageing process.[20]

We examined how oxidative stress affects the permeability and cytoskeleton and barrier protein expression of AAP cells. Cytoskeletal proteins and cell–cell junction proteins are important in maintaining the barrier function and permeability of cell layers. In the case of glaucoma, the alteration of the expressions and organization of these proteins may lead to decrease in aqueous humor outflow and increase in IOP.[21] Among these proteins, we chose to investigate those that are involved in actomyosin organization and cell–cell junctions, including F-actin, β-catenin, myosin light chain, occludin, claudin-5, ZO-1, and VE-cadherin.

Materials and Methods

Materials

Porcine eyes were obtained from a local abattoir within 8 hours postmortem and were stored in a fridge in Hanks balanced salt solution supplemented with 200 U/mL penicillin, 200 μg/mL streptomycin, 5 μg/mL amphotericin B, and 100 μg/mL gentamycin.

Dulbecco's modified Eagle's medium (DMEM), endothelial cell growth factor, newborn calf serum, heparin, penicillin, streptomycin, amphotericin, gentamycin, 2% gelatin, phosphate-buffered saline (PBS), sterile Hanks balanced salt solution with sodium bicarbonate, ×1 trypsin EDTA solution and Triton X-100, Collagenase I, Hoechst 33258, potassium ferricyanide ($K_3Fe(CN)_6$) and 30 mM potassium ferrocyanide ($K_4Fe(CN)_6{\cdot}3H_2O$), and 1 mM $MgCl_2$ were all purchased from Sigma (Shanghai, China). Cell strainer (40 μm) was from Becton and Dickinson Falcon (Shanghai, China). Platelet poor plasma derived serum was sourced from Biomedical Technologies Inc. (Stoughton, MA). Puromycin was from Invivo Gen (San Diego, CA).

Cell Isolation and Culture

AAP endothelial cells were isolated according to an established method reported by our group.[22] Briefly, for each strain of cells, the TM tissue (including AAP vessels) was dissected from six porcine eyes (four quadrants per eye, 4- to 6-month-old pigs) and pooled to generate a primary mixed cultures of porcine TM and AAP cells following collagenase I (1 mg/mL; Sigma) digestion. Cells were then allowed to multiply until they were nearly confluent (typically 8 days), and then treated by 4 μg/mL of puromycin for 2 days. AAP cells were selected from TM cells using puromycin treatment. The cultures were allowed to recover and the remaining cells to populate.

Experimental Model of Chronic Oxidative Stress in Porcine SC Cells

Chronic oxidative stress was induced according to an established method used to study the ageing of TM cells.[15] In brief, porcine SC cells were subjected to normobaric hyperoxia conditions. Porcine SC cells at passage 1 were grown for 14 days at 40% O_2 and 5% CO_2 in a triple-gas incubator (Smart Cell, Shanghai, China). Control cultures were grown under physiological oxygen conditions (5% O_2, 5% CO_2).

Cell Growth Rate

Cells were seeded into 24-well plates (Corning, Shanghai, China) at a density of 1×10^4 cells/cm^2. AAP cells were cultured in high oxygen (40%) condition for 1 to 14 days, and the cells were trypsinized and stained with 0.5% trypan blue solution, and counted using Countess Automated Cell Counter (Invitrogen, Shanghai, China). Cells from four cells strains were tested, with three replicates for each day.

Cell Size

After the oxidative stress period, cells were trypsinized and subcultured. The next day, cells were imaged in randomly selected locations ($n = 20$ in each sample). The size of selected cells was measured using ImageJ software (National Institutes of Health [NIH], Bethesda, MD). Six independent lines of cells were measured for each group.

β-Galactosidase Assay

Cells were stained for a senescence marker, β-galactosidase, following an established protocol.[23] Preconfluent cells (~80%) grown in six-well plates were first washed in PBS three times (30 seconds each time). Cells were then fixed in 2% paraformaldehyde (PFA) and 0.2% glutaraldehyde solution (v/v) for 5 minutes at room temperature, and were washed three times in PBS (30 seconds each time). A solution was made containing 30 mM potassium ferricyanide ($K_3Fe(CN)_6$), 30 mM potassium ferrocyanide ($K_4Fe(CN)_6{\cdot}3H_2O$), 1 mM $MgCl_2$, and 1 mg/mL Xgal in PBS at pH 6. One milliliter of this solution was added to each well of cells and incubated overnight (12–16 hours) at 37°C. After the incubation, cells were washed three times with PBS (30 seconds each time) and once with methanol. The plates were allowed to dry and stained cells were viewed by phase contrast microscopy (Leica, Shanghai, China).

DNA Damage

Cells were stained for 8-hydroxy-2′-deoxyguanosine (8-OHdG), an oxidative damage marker of cellular DNA. Cells were fixed in 4% PFA overnight at room temperature, and were washed three times in PBS (pH 7.2, 10 minutes each time). Endogenous peroxidase activity was neutralized by incubating cells in 1% H_2O_2 in methanol for 20 minutes and washed with PBS. Nonspecific binding sites on cells were blocked in 1% BSA solution for 1 hour at room temperature and permeabilized with 0.2% Triton X-100 for 5 minutes. Cells were then incubated with 8-hydroxyguanosine antibody (goat polyconal, 1:200; Abcam, Shanghai, China) overnight at 4°C. Cells were washed three times in PBS (10 minutes each time) then incubated with rabbit anti-goat biotin-conjugated secondary antibody (1:1000 dilution; Abcam) in PBS for 30 minutes at room temperature. Celled were rinsed in PBS three times (10 minutes each time), and incubated in streptavidin-biotin solution (1:500 dilution; Invitrogen) in PBS for 30 minutes at room temperature. After cells were rinsed in PBS for three times (5 minutes each time), they were incubated in DAB enhanced substrate system (Sigma-Aldrich, Shanghai, China) for 5 minutes, and rinsed three times again in PBS.

Transendothelial Electrical Resistance

Transendothelial electrical resistance (TEER) measurements across confluent AAP cell monolayers grown on transwells

Investigative Ophthalmology & Visual Science

were performed at room temperature with STX-2 Ag/AgCl electrodes and an EVOM2 Voltohmeter (World Precision Instruments, Shanghai, China) according to manufacturer's instructions. This method of measuring TEER has previously been used by many groups in the microvascular field and several groups in the glaucoma field.[11,21,24,25] Briefly, the electrode was placed inside the well, which allowed the longer (external) electrode to touch the bottom of the dish containing the external culture media while preventing the shorter (internal electrode) from reaching the bottom of the cell culture insert. Ten measurements were taken per each well, and three 12-well plates were measured for each strain of cells. In the same experimental group, the electrode was not rinsed when moving from one sample cup to another to avoid resistant measurement drift. However, the electrode was rinsed with culture media between measurements to avoid carryover of one sample into the next. All measurements of TEER were corrected to account for the resistance of the filter membrane. The result was expressed in units of ohms $\times$ cm^2. Three wells of cells were measured per cell strain, and six strains of cells were measured from each group.

Hydraulic Conductivity

Confluent cell monolayers were perfused in the apical to basal direction and hydraulic conductivity (HC) measured using an established protocol.[26] Our perfusion set-up was adapted from a previously described system by our group.[27] Briefly, it consists of a computer-controlled syringe pump that adjusts the flow rate (Q) across the cell layer to maintain a user-defined pressure drop (ΔP), a silicon stopper, and transwell. AAP cells were seeded onto the bottom or bottom-facing surface of a transwell permeable filter membrane insert at a density of 4×10^4 cells/cm^2 (Corning 3460; 0.4-μm track-etch pore diameter, 12-mm membrane diameter; 4×10^6 pores/cm^2) and cultured until the culture was confluent. In our experience, TEER of the SC monolayer became stable after approximately 4 to 6 days after seeding. HC was measured when TEER was stable for three consecutive days. Cells were perfused at a pressure drop of 4 mm Hg for 20 minutes after the pressure became stable. The expected pressure drops across the inner wall of SC in vivo is in the range of 2 and 6 mm Hg. Hydraulic conductivity (Lp) was calculated from $Lp = Q/(\Delta P \times A)$, where A is the membrane area).

Immunofluorescence Labeling

Protein expression was analyzed by immunolabeling for phalloidin, occludin, β-catenin, and phosphorylated myosin light chain, claudin-5, and ZO-1. Cells were seeded onto glass coverslips that were precoated with 2% gelatin solution at confluence and after cultured for 14 days in normal or high levels of oxygen. Cells were fixed with 4% formaldehyde overnight and then washed three times with PBS. Nonspecific binding sites on cells were blocked in goat serum for 1 hour at room temperature and permeabilized with 0.2% Triton X-100 for 5 minutes. Cells were then incubated with phalloidin (1:1000; Abcam), antibodies against occludin (1:400; Abcam), β-catenin (1:400; Abcam), myosin light chain (phospho S20, 1:200; Abcam), claudin (1:200; Abcam), ZO-1 (1:100; Abcam), and VE-cadherin (1:200; Abcam) overnight at 4°C. After three washes with PBS, cells were incubated in secondary antibody (Alexa Fluor 488, goat anti-rabbit) and Hochst 33258 solution (0.5 μg/mL; Sigma).

Western Blot

Cell lysates were prepared using RIPA solution containing 1% Igepal CA-630, 0.5% sodium deoxycholate, and 0.1% SDS in PBS. Protein concentration was estimated by the Bradford method. Equal amounts of protein (50 μg protein/lane) were separated by SDS-PAGE (10% or 12.5% acrylamide), followed by electrophoretic transfer of resolved proteins to nitrocellulose filters. The membrane was blocked by 5% nonfat dry milk in Tris-buffered saline with 0.05% Tween-20 for 2 hours. Filters were then probed using primary antibodies specifically directed against occludin (1:200; Abcam), β-catenin (1:4000; Abcam), myosin light chain (1:1000; Abcam), claudin (1:500; Abcam), ZO-1 (1:50; Abcam), and VE-cadherin (1:500; Abcam) followed by incubation with peroxidase-linked secondary antibodies. Detection of immunoreactivity was carried out by enhanced chemiluminescence according to manufacturer's recommendations. GAPDH was used as a loading control. Signals in the linear range of the X-ray film were captured digitally and densitometry performed using Molecular Imaging Software (Carestream Health, Beijing, China).

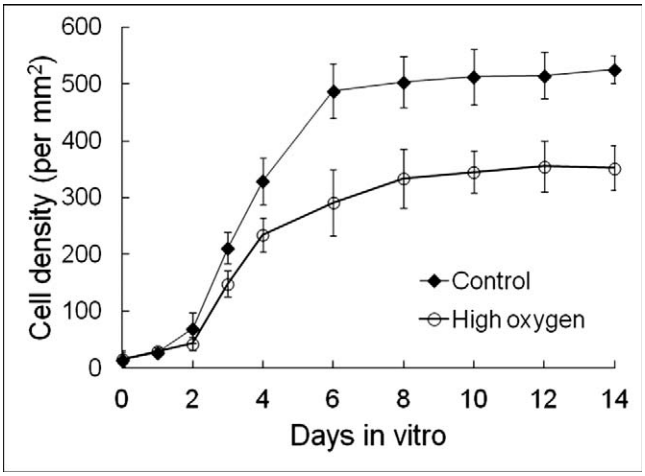

Figure 1. Growth curves (mean ± standard deviation) for AAP cells cultured in normal oxygen and high oxygen conditions ($n = 3$ replicates of experiment using four different cell strains).

Statistics

For TEER and HC measurements, data distribution normality was first tested. And data was analyzed by the Mann-Whitney U test (SPSS 17 for Windows; IBM SPSS, Chicago, IL). In all cases, differences were considered significant at $P < 0.05$.

Results

Porcine AAP cells were isolated away from other cells in conventional outflow pathway according to an established method by our laboratory using puromycin treatment.[22] Over 90% of the cells were killed by puromycin treatment for 48 hours, leaving cells with an endothelial appearance.

To study the effects of hyperoxia on cultured AAP cell monolayers, we first investigated cell growth rate and markers for senescence. Our data showed that chronic hyperoxia significantly impacted cell growth from day 3 onwards (Fig. 1). After 14 days of high oxygen exposure, the cell number was only approximately 67% of control. Correspondingly, oxidative stress caused a significant increase in cell size, which was 18.2% ± 5.1% higher than control ($P < 0.05$, Figs. 2A, 2B). Moreover, cells in the hyperoxia group stained positive for the ageing marker β-galactosidase and the DNA damage marker 8-OHdG (Figs. 2D, 2F), suggesting that the chronic hyperoxia model rendered AAP cells prone to senescence and cellular

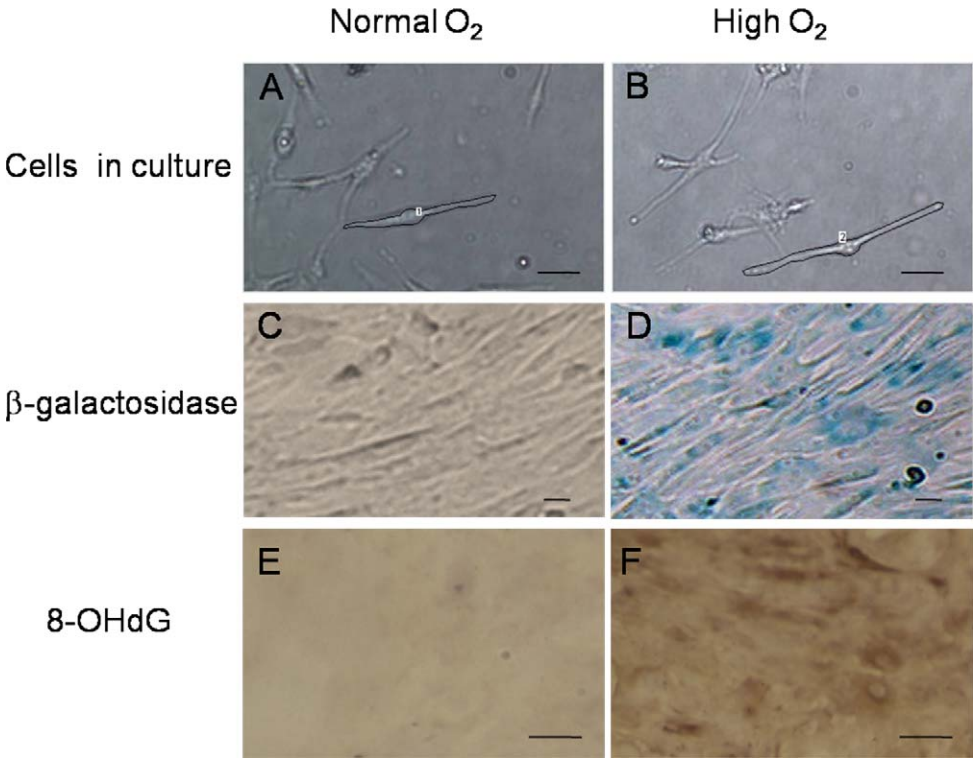

Figure 2. AAP cells cultured in control and in high oxygen conditions. Hyperoxia resulted in an increase in cell size compared to control (**A**) versus (**B**), which was later quantified to be an 18.2% increase. *Polygonal shape outlines* show an example of the measurements; *outlines* are labeled *1* in (**A**) and *2* in (**B**). When cells were stained for senescence marker β-galactosidase, those cultured under normal conditions had negligible staining for β-galactosidase (**C**), whereas cells cultured in high oxygen condition stained positive for the ageing marker (**D**). (**E**, **F**) Cells grown in normal and high oxygen conditions, respectively, which were stained for the DNA damage marker 8-OHdG. Cell under oxidative stress have increased staining for 8-OHdG compared to cells grown in normal oxygen conditions. *Scale bar*: 40 μm.

DNA damage. In contrast, the AAP cells cultured for the same period of time but in normal oxygen did not show positive staining for either the ageing marker or the DNA damage marker (Figs. 2C, 2E).

Oxidative stress affected two different measurements of AAP barrier function. When perfused in the basal-to-apical direction at 4 mm Hg, HC of AAP cells was 28% higher in hyperoxia group compared to control (1.97 ± 0.12 vs. 1.54 ± 0.13 μL/mm Hg/min/cm^2, $P < 0.05$, $n = 6$, Fig. 3C). Similarly, TEER in the hyperoxia group was significantly higher compared with the control group from day 10 onwards; by 27.5%, 31.2%, and 31.3% on day 10, 12, and 14, respectively ($P < 0.05$, $n = 6$, Fig. 4). Control monolayers reached a stable net TEER of ~27 Ω·cm^2, while net TEER of cells exposed to hyperoxia continued to climb, stabilizing around day 10 at ~37 Ω·cm^2. In our hands TEER was more variable when cells were not completely confluent, but it became more stable as cells reached confluence (Fig. 4) and the difference in TEER was statistically significant ($P < 0.05$) when cells were confluent and TEER was stable. The values that we obtained were consistent with those reported previously for human and primate SC cells.[11,21,24,25]

We examined the AAP cells more closely, looking for molecular contributors to increased barrier behavior. Using immunofluorescence microscopy, we examined the distribution and qualitative abundance of proteins known to contribute to barrier function in endothelia. Results showed that the cells exposed to oxidative stress qualitatively expressed an overall greater abundance of F-actin (Figs. 5A–C), MLC phospho (Figs. 5D–F), occludin (Figs. 5G–I), claudin-5 (Figs. 5J–L), β-catenin (Figs. 5M–O), and VE-cadherin (Figs. 5P–R) compared to the control group. At the site of cell–cell contact, we also observed increased expression of F-actin, β-catenin, and VE-cadherin. Interestingly, we did not observe an increased distribution of occludin at these sites. ZO-1 expression was not detected with immunostaining (the staining was performed four times each with two different batches of antibody), which may have been due to the incompatibility of the antibody with the staining method or species of cells.

For a better quantitative assessment, levels of candidate proteins were analyzed via Western blot. Comparisons were made using equal protein loadings of AAP cell lysates to a single gel and compared to GAPDH expression. As before, a greater expression level of phospho-MLC, occludin, claudin-5, ZO-1, β-catenin, and VE-cadherin was observed in the hyperoxia cells compared to the controls in all six cell strains of each group tested (Fig. 6A). Densitometry analysis showed that the expression of phospho-MLC, occludin, claudin-5, ZO-1, β-catenin, and VE-cadherin increased by 2.17 ± 0.45 fold, 1.238 ± 0.21 fold, 1.83 ± 0.42 fold, 3.90 ± 0.87 fold, 2.74 ± 1.06 fold, and 4.54 ± 1.21 fold, respectively (Fig. 6B).

Discussion

Here we used chronic hyperoxia as a model for ageing to study effects on AAP function and expression of proteins involved in cell–cell adhesion. This model successfully induced cell senescence as the stressed cells were positive for the cell senescence marker β-galactosidase and the DNA damage marker 8-OHdG and had reduced growth rate. Our data showed that chronic oxidative stress rendered the AAP cells more resistant to paracellular fluid flow as demonstrated in higher TEER and lower hydraulic conductivity measurements.

Investigative Ophthalmology & Visual Science

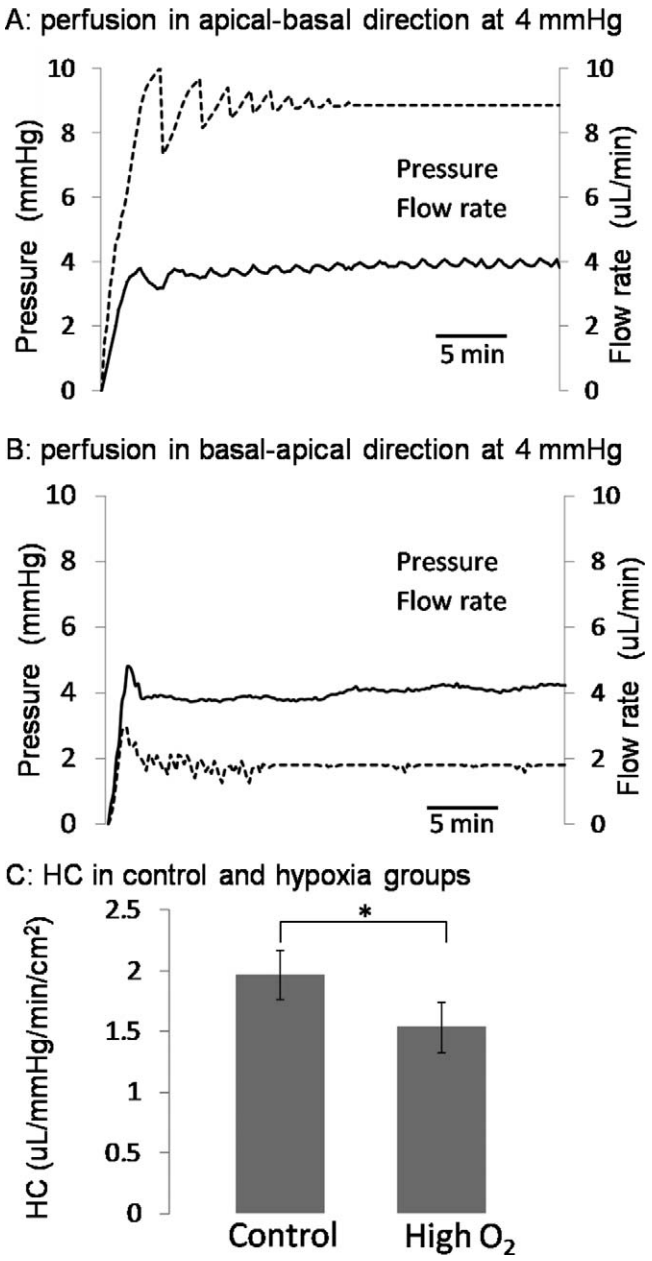

FIGURE 3. Hydraulic conductivity (HC) of AAP cell monolayers. The cells were cultured on the bottom-facing surface of a transwell membrane and perfused in the apical-basal (**A**) or basal-to-apical (**B**) direction. The flow rate across the cell layer was set by a computer-controlled syringe pump to maintain a specified pressure drop. (**A**, **B**) Representative pressure (*solid curve*; *left axis*) and flow (*dashed curve*; *right axis*) traces for perfusions at a constant pressure of 4 mm Hg. (**C**) Bar plot showing summary of HC data in control and high oxygen groups perfused in the apical to basal direction. HC was significantly lower in hyperoxia group compared with control. *Error bar* is standard deviation; $^{*}P < 0.05$.

The increased resistance of AAP cells coincided with increase in cell size, senescence marker, actin and actomyosin reorganization, and tight junction, as well as adhesion junction protein expression levels. Taken together, we for the first time show that chronic oxidative stress increases barrier function of AAP cells and abundance or localization of several junction-associated proteins known to regulate paracellular permeability.

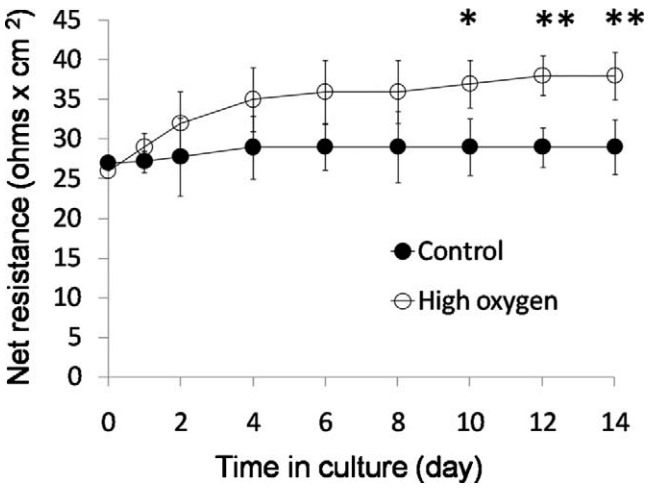

FIGURE 4. Changes in net TEER in the AAP endothelial cell monolayers. AAP cells were cultured in normal oxygen and 40% oxygen for 14 days. In the hyperoxia group, the net resistance was significantly higher from day 10 to day 14 compared with control ($^{*}P < 0.05$, $^{**}P < 0.01$, $n = 6$ for each time point).

AAP is the functional equivalent of human SC. It facilitates the drainage of aqueous humor from the eye into the systemic circulation. The monolayer of cells that form AAP venous vessels develop pressure-dependent outpouchings into their lumen (giant vacuoles), providing evidence of fluid flow and pressure-drop across the endothelia. The cells in both species are also a key part of the blood-aqueous barrier, maintaining intraocular immune privilege and keeping blood products from entering the eye from the venous system during times of elevated episcleral venous pressure.

Porcine eyes are a good model for human eyes[28,29] as a model for studying glaucoma,[15,28,30,31] aqueous humor outflow physiology,[31–33] and chronic IOP elevation,[28,29] and similar to human, outflow facility in both is reduced in response to TGF-β_2.[32] Porcine TM cells are already widely used by glaucoma researchers as a surrogate for human TM cells. In this study we employed an established method of isolating AAP cells published by our group previously.[34] The cells we isolated are AAP cells for the following reasons. First, the selected AAP cells displayed fusiform morphology as individual cells and take on a cobble stone morphology at confluence as reported previously.[22] Second, the selected AAP cells exhibited contact inhibition upon reaching confluence, consistent with the behavior reported for human SC cells (Fig. 2) and other endothelia. Third, cells expressed the same surface markers as those seen in cultured human SC cells and in AAP of intact porcine tissue, including the typical endothelial markers VE-cadherin, vWF, and ICAM II, but were negative for α-smooth muscle actin as reported previously.[22] Fourth, hydraulic conductivity of selected cells is significantly different when perfused from basal-to-apical and apical-to-basal directions, which is characteristic of human SC cells. Also the values reported are similar to human SC cells,[26] which are 1.97 ± 0.13 ($n = 6$) and 0.39 ± 0.01 ($n = 6$) μL/mm Hg/min/cm^2 when perfused from apical to basal and basal to apical direction at 4 mm Hg, respectively.

Age-related changes in the SC endothelial inner wall have been demonstrated in several studies. Boldea et al.[35] showed that SC inner wall filtration function was significantly influenced by age. Moreover, SC size, endothelial cell population, pores, and vacuoles decreased with age.[35–37] Regression analyses estimate the loss of SC cells to be on the order of 430 cells per year for the whole canal.[36] Further, a

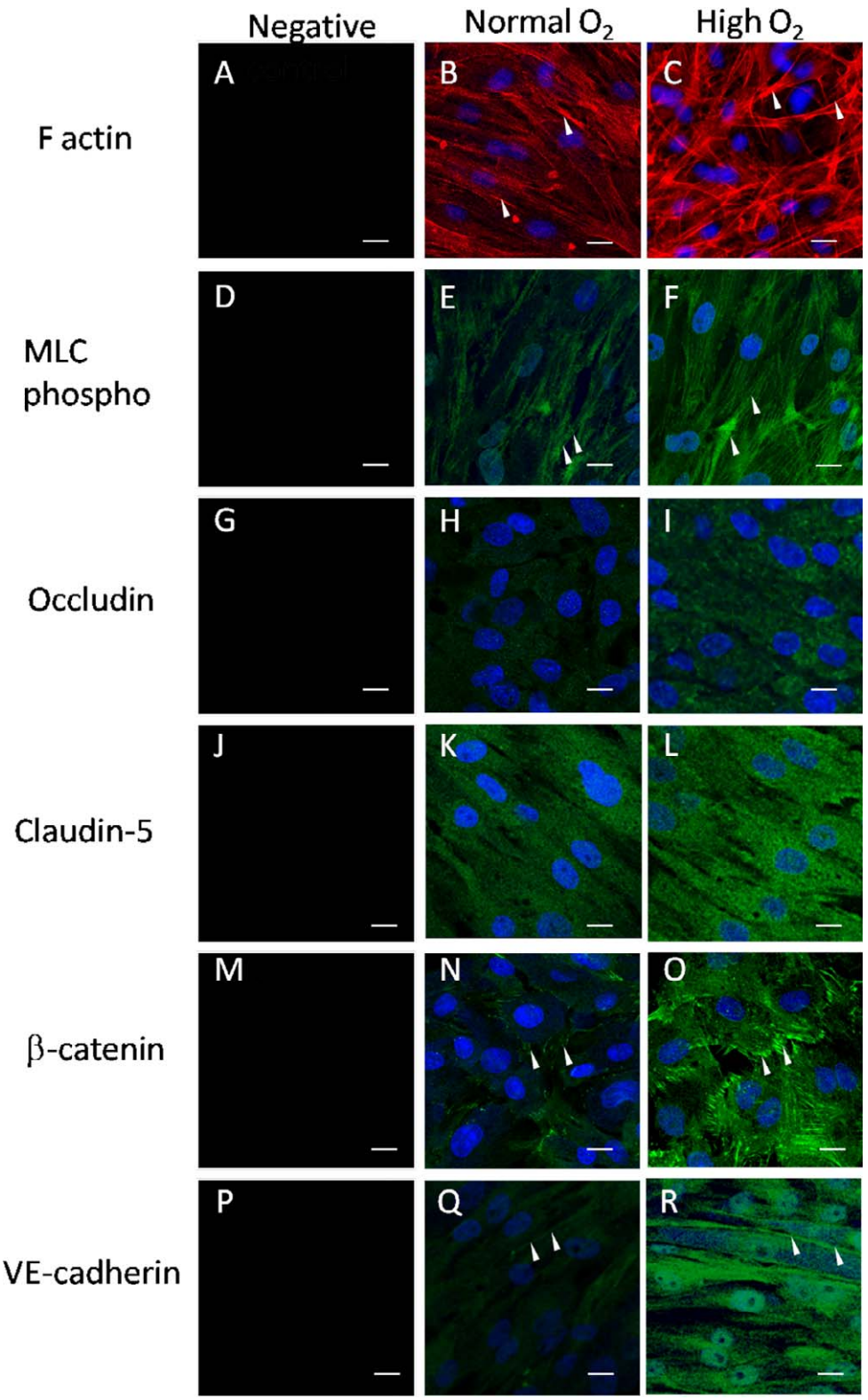

Figure 5. Expression of cytoskeletal and cell–cell adhesion proteins by AAP cells monitored by immunofluorescence microscopy. The expression of F-actin (**A–C**), myosin light chain phospho (**D–F**), occludin (**G–I**), claudin-5 (**J–L**), and β-catenin (**M–O**), VE-cadherin (**P–R**) appeared higher in high oxygen group compared with normal oxygen group. Background labeling was monitored via omission of primary antibody and DAPI (*first column*). Shown are representative images of one experiment of six in total. All the images are shown at the same magnification, gain, and offset settings. At the site of cell–cell contact, we also observed increased expression of F-actin, β-catenin, and VE-cadherin as indicated by *arrowheads*. *Scale bar*: 10 μm.

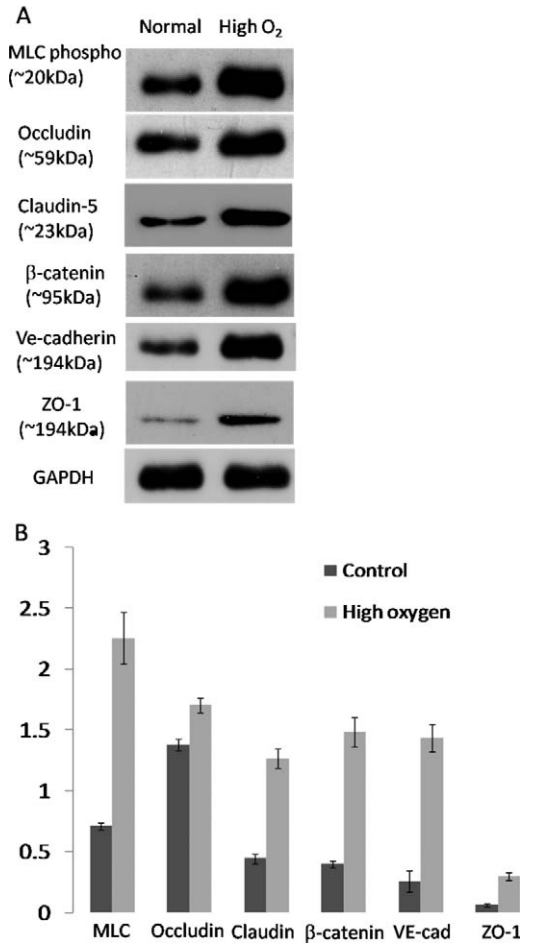

Figure 6. Western blot analysis of barrier protein expression by AAP cells under normal and hyperoxic conditions. (**A**) Representative Western blots of MLC phospho, occludin, claudin, ZO-1, β-catenin, and VE-cadherin and (**B**) densitometric analysis of blots (mean ± standard deviation of the mean). *Y*-axis is the blot density ratio of protein and GADPH. Shown are representative images of one experiment of six in total.

number of other age-related changes in the aqueous humor dynamics have been reported, such as the decline in the rate of aqueous production,[38–40] episclera venous pressure,[41] ocular rigidity,[42] and accumulation of extracellular material in the conventional and unconventional outflow pathways.[43–46] Studies in nonglaucomatous humans demonstrated that total outflow facility decreases with age.[41] Being exposed to a high oxygen culture condition for 14 days, AAP cells stained positive for ageing marker β-galactosidase (Fig. 2), which is a known marker of senescent cells not found in presenescent, quiescent, or immortal cells. Oxidative stress also caused cell DNA damage as revealed by 8-OHdG staining, which is marker of oxidative damage in cellular DNA. Here, we confirmed that ageing of AAP cells resulted in changes of cell size and resistance to outflow in our model (Figs. 3, 4).

Functional evaluation showed that HC and TEER of AAP cells was significantly higher in the hyperoxia group compared to the control. Although the TEER measurements are routinely used as an endpoint measure by many in the microvascular field and several in the glaucoma field,[11,23,26,27] they only give an indication of the maturity of cell–cell adhesions under different in vitro conditions, modeling possible cellular responses in vivo.

At the site of cell–cell contact, we observed increased expression of F-actin, β-catenin, and VE-cadherin under oxidative stress, but not occludin or claudin-5 (Figs. 5G–L), which only had an overall up regulation of protein but not redistribution to cell–cell contacts (Figs. 5, 6). This may be due to the down-regulation of these proteins in vitro. In contrast, human umbilical vein endothelial cells (HUVECs) showed down-regulation of occludin and claudin-5, and little difference in VE-cadherin and ZO-1 expression in their senescent state.[47] This may be due to the difference in the properties of the cells. For example, HUVECs are derived from large veins, whereas AAP cells are from microvascular veins. AAP cells experience very different biomechanical stimuli from HUVECs[48]; that is, HUVEC cells experience shear stress and stretch,[48] whereas AAP cells experience pressure drop from a basal-to-apical direction. Others also noted differences in the dynamic process involved in giant vacuole formation.[26]

Ageing of vascular endothelial cells contributing to the pathogenesis and progression of diseases is not unique to glaucoma. In cardiovascular diseases such as atherosclerosis, ageing of the vascular endothelial cells is thought to be important in the pathogenesis and progression.[49] Apart from the alterations related to cell replication blockade, there are also changes in gene expression, morphology, and function.[50,51] Advanced age also leads to decrease of endothelial NO production. Some studies found that senescent endothelial cells have lower levels of endothelial NO synthase (eNOS) activity and produce decreased levels of NO.[52] Furthermore, the effect of shear stress, which induces eNOS expression, was markedly blunted in senescent endothelial cells. Recent data by our group show that eNOS expression by mouse SC cells may be important in regulating outflow facility.[48] Our data confirmed that ageing impaired permeability of the AAP cells, resulting in an increased resistance to aqueous flow. This could be explained by an increased level of expression of barrier proteins and the reorganization of actin and actomyosin. In future studies, it will be interesting to see if other functions like NO production by senescent AAP cells are compromised.

Conclusions

While the physiology of AAP cells is not known, our data showed that oxidative stress caused by hyperoxic conditions, as a model of ageing, induces molecular changes to barrier function in monolayer AAP cells.

Acknowledgments

We thank Huang Yalin from the Stem Cell Research Centre of Fudan University for her technical support in confocal imaging.

Supported by Eye and ENT Hospital Research Fund, National Science Foundation China (81100662), Fundamental Research Funds for the Central Universities, Science and Technology Commission of Shanghai (11PJ1402100), 211 Project of Fudan University (EHF158351), Allergen Unlimited Research Fund, EY022359 (WDS), and Research to Prevent Blindness Foundation (WDS).

Disclosure: **Y. Lei**, Allergan (F); **W.D. Stamer**, None; **J. Wu**, None; **X. Sun**, None

References

1. Quigley HA, Broman AT. The number of people with glaucoma worldwide in 2010 and 2020. *Br J Ophthalmol*. 2006;90:262–267.
2. Friedman DS. Prevalence of open-angle glaucoma among adults in the United States. *Archives of Ophthalmology*. 2004;122:532–538.

3. Repka MX, Quigley HA. The effect of age on normal human optic nerve fiber number and diameter. *Ophthalmology*. 1989; 96:26–32.
4. Drance S, Anderson DR, Schulzer M. Risk factors for progression of visual field abnormalities in normal-tension glaucoma. *Am J Ophthalmol*. 2001;131:699–708.
5. Mason RP, Kosoko O, Wilson MR, et al. National survey of the prevalence and risk factors of glaucoma in St. Lucia, West Indies. Part I. Prevalence findings. *Ophthalmology*. 1989;96: 1363–1368.
6. Leske MC, Connell AM, Schachat AP, Hyman L. The Barbados Eye Study. Prevalence of open angle glaucoma. *Arch Ophthalmol*. 1994;112:821–829.
7. Wensor MD, McCarty CA, Stanislavsky YL, Livingston PM, Taylor HR. The prevalence of glaucoma in the Melbourne Visual Impairment Project. *Ophthalmology*. 1998;105:733–739.
8. Tielsch JM, Sommer A, Katz J, Royall RM, Quigley HA, Javitt J. Racial variations in the prevalence of primary open-angle glaucoma: the Baltimore eye survey. *J AM MED ASSOC*. 1991; 266:369–374.
9. Green K. Free radicals and aging of anterior segment tissues of the eye: a hypothesis. *Ophthalmic Res*. 1995;27(Suppl 1);143–149.
10. Wang N, Chintala SK, Fini ME, Schuman JS. Activation of a tissue-specific stress response in the aqueous outflow pathway of the eye defines the glaucoma disease phenotype. *Nat Med*. 2001;7:304–309.
11. Stamer WD, Roberts BC, Epstein DL. Hydraulic pressure stimulates adenosine 3′, 5′-cyclic monophosphate accumulation in endothelial cells from Schlemm's canal. *Invest Ophthalmol Vis Sci*. 1999;40:1983–1988.
12. Rosenquist R, Epstein D, Melamed S, Johnson M, Grant WM. Outflow resistance of enucleated human eyes at two different perfusion pressures and different extents of trabeculotomy. *Curr Eye Res*. 1989;8:1233–1240.
13. Underwood JL, Murphy CG, Chen J, et al. Glucocorticoids regulate transendothelial fluid flow resistance and formation of intercellular junctions. *Am J Physiol*. 1999;277:C330–342.
14. Ethier CR, Chan DW. Cationic ferritin changes outflow facility in human eyes whereas anionic ferritin does not. *Invest Ophthalmol Vis Sci*. 2001;42:1795–1802.
15. Liton PB, Lin Y, Luna C, Li G, Gonzalez P, Epstein DL. Cultured porcine trabecular meshwork cells display altered lysosomal function when subjected to chronic oxidative stress. *Invest Ophthalmol Vis Sci*. 2008;49:3961–3969.
16. Sitte N, Huber M, Grune T, et al. Proteasome inhibition by lipofuscin/ceroid during postmitotic aging of fibroblasts. *FASEB J*. 2000;14:1490–1498.
17. Terman A, Brunk UT. Ceroid/lipofuscin formation in cultured human fibroblasts: the role of oxidative stress and lysosomal proteolysis. *Mech Ageing Dev*. 1998;104:277–291.
18. Zheng L, Roberg K, Jerhammar F, Marcusson J, Terman A. Oxidative stress induces intralysosomal accumulation of Alzheimer amyloid beta-protein in cultured neuroblastoma cells. *Ann N Y Acad Sci*. 2006;1067:248–251.
19. Liton PB, Lin Y, Luna C, Li G, Gonzalez P, Epstein DL. Cultured porcine trabecular meshwork cells display altered lysosomal function when subjected to chronic oxidative stress. *Invest Ophthalmol Vis Sci*. 2008;49:3961–3969.
20. Finkel T, Holbrook NJ. Oxidants, oxidative stress and the biology of ageing. *Nature*. 2000;408:239–247.
21. Kameda T, Inoue T, Inatani M, et al. The effect of Rho-associated protein kinase inhibitor on monkey Schlemm's canal endothelial cells. *Invest Ophthalmol Vis Sci*. 2012;53:3092–3103.
22. Lei Y, Overby DR, Read AT, Stamer WD, Ethier CR. A new method for selection of angular aqueous plexus cells from porcine eyes: a model for Schlemm's canal endothelium. *Invest Ophthalmol Vis Sci*. 2010;51:5744–5750.
23. Debacq-Chainiaux F, Erusalimsky JD, Campisi J, Toussaint O. Protocols to detect senescence-associated beta-galactosidase (SA-betagal) activity, a biomarker of senescent cells in culture and in vivo. *Nat Protoc*. 2009;4:1798–1806.
24. Alvarado JA, Betanzos A, Franse-Carman L, Chen J, Gonzalez-Mariscal L. Endothelia of Schlemm's canal and trabecular meshwork: distinct molecular, functional, and anatomic features. *Am J Physiol Cell Physiol*. 2004;286:C621–634.
25. Ellis DZ, Sharif NA, Dismuke WM. Endogenous regulation of human Schlemm's canal cell volume by nitric oxide signaling. *Invest Ophthalmol Vis Sci*. 2010;51:5817–5824.
26. Pedrigi RM, Simon D, Reed A, Stamer WD, Overby DR. A model of giant vacuole dynamics in human Schlemm's canal endothelial cells. *Experimental Eye Research*. 2011;92:57–66.
27. Lei Y, Overby DR, Boussommier-Calleja A, Stamer WD, Ethier CR. Outflow physiology of the mouse eye: pressure dependence and washout. *Invest Ophthalmol Vis Sci*. 2011;52: 1865–1871.
28. Ruiz-Ederra J, Garcia M, Hernandez M, et al. The pig eye as a novel model of glaucoma. *Exp Eye Res*. 2005;81:561–569.
29. McMenamin PG, Steptoe RJ. Normal anatomy of the aqueous humour outflow system in the domestic pig eye. *J Anat*. 1991; 178:65–77.
30. Shaarawy T, Wu R, Mermoud A, Flammer J, Haefliger IO. Influence of non-penetrating glaucoma surgery on aqueous outflow facility in isolated porcine eyes. *Br J Ophthalmol*. 2004;88:950–952.
31. Epstein DL, Rowlette LL, Roberts BC. Acto-myosin drug effects and aqueous outflow function. *Invest Ophthalmol Vis Sci*. 1999;40:74–81.
32. Bachmann B, Birke M, Kook D, Eichhorn M, Lutjen-Drecoll E. Ultrastructural and biochemical evaluation of the porcine anterior chamber perfusion model. *Invest Ophthalmol Vis Sci*. 2006;47:2011–2020.
33. Yan DB, Trope GE, Ethier CR, Menon IA, Wakeham A. Effects of hydrogen peroxide-induced oxidative damage on outflow facility and washout in pig eyes. *Invest Ophthalmol Vis Sci*. 1991;32:2515–2520.
34. Lei Y, Overby D, Read T, Stamer WD, Ethier CRA. New method for selection of angular aqueous plexus cells from porcine eyes: a model for Schlemm's canal endothelium. *Invest Ophthalmol Vis Sci*. 2010;51:5744–5750.
35. Boldea RC, Roy S, Mermoud A. Ageing of Schlemm's canal in nonglaucomatous subjects. *Int Ophthalmol*. 2001;24:67–77.
36. Grierson I, Howes RC, Wang Q. Age-related changes in the canal of Schlemm. *Exp Eye Res*. 1984;39:505–512.
37. Ainsworth JR, Lee WR. Effects of age and rapid high-pressure fixation on the morphology of Schlemm's canal. *Invest Ophthalmol Vis Sci*. 1990;31:745–750.
38. Bloom JN, Levene RZ, Thomas G, Kimura R. Fluorophotometry and the rate of aqueous flow in man. I. Instrumentation and normal values. *Arch Ophthalmol*. 1976;94:435–443.
39. Becker B. The decline in aqueous secretion and outflow facility with age. *Am J Ophthalmol*. 1958;46:731–736.
40. Brubaker RF, Nagataki S, Townsend DJ, Burns RR, Higgins RG, Wentworth W. The effect of age on aqueous humor formation in man. *Ophthalmology*. 1981;88:283–288.
41. Toris CB, Yablonski ME, Wang YL, Camras CB. Aqueous humor dynamics in the aging human eye. *Am J Ophthalmol*. 1999; 127:407–412.
42. Gabelt BT, Kaufman PL. Changes in aqueous humor dynamics with age and glaucoma. *Prog Retin Eye Res*. 2005;24:612–637.
43. Miyazaki M, Segawa K, Urakawa Y. Age-related changes in the trabecular meshwork of the normal human eye. *Jpn J Ophthalmol*. 1987;31:558–569.

Investigative Ophthalmology & Visual Science

44. Alvarado J, Murphy C, Polansky J, Juster R. Age-related changes in trabecular meshwork cellularity. *Invest Ophthalmol Vis Sci*. 1981;21:714–727.

45. Tamm E, Croft MA, Jungkunz W, Lutjen-Drecoll E, Kaufman PL. Age-related loss of ciliary muscle mobility in the rhesus monkey. Role of the choroid. *Arch Ophthalmol*. 1992;110: 871–876.

46. Tamm S, Tamm E, Rohen JW. Age-related changes of the human ciliary muscle. A quantitative morphometric study. *Mech Ageing Dev*. 1992;62:209–221.

47. Krouwer VJ, Hekking LH, Langelaar-Makkinje M, Regan-Klapisz E, Post JA. Endothelial cell senescence is associated with disrupted cell-cell junctions and increased monolayer permeability. *Vascular cell*. 2012;4:12.

48. Stamer WD, Lei Y, Boussommier-Calleja A, Overby DR, Ethier CR. eNOS, a pressure-dependent regulator of intraocular pressure. *Invest Ophthalmol Vis Sci*. 2011;52:9438–9444.

49. Erusalimsky JD, Kurz DJ. Endothelial cell senescence. *Handb Exp Pharmacol*. 2006;(176 Pt 2):213–248.

50. Minamino T, Miyauchi H, Yoshida T, Komuro I. [Endothelial cell senescence in human atherosclerosis: role of telomeres in endothelial dysfunction]. *J Cardiol*. 2003;41:39–40.

51. Minamino T, Miyauchi H, Yoshida T, Ishida Y, Yoshida H, Komuro I. Endothelial cell senescence in human atherosclerosis: role of telomere in endothelial dysfunction. *Circulation*. 2002;105:1541–1544.

52. Matsushita H, Chang E, Glassford AJ, Cooke JP, Chiu CP, Tsao PS. eNOS activity is reduced in senescent human endothelial cells: preservation by hTERT immortalization. *Circ Res*. 2001; 89:793–798.

Investigative Ophthalmology & Visual Science